12th AIAA/ISSMO Multidisciplinary Analysis and Optimization Conference
10 - 12 September 2008, Victoria, British Columbia Canada

AIAA 2008-5997

Influence of Selection Criterion on RBF Topology Selection for Crashworthiness Optimization

Tushar Goel[1], Nielen Stander[2]

Livermore Software Technology Corporation, Livermore CA 94551

The performance of radial basis function networks largely depends on the choice of topology i.e., location and number of centers, radius of influence. Thus finding the best network is a multi-level optimization problem. It is obvious that different criteria for optimization would result in different network topologies. A systematic study is carried out to compare the most widely used root mean square error criterion for topology selection with cross-validation based methods like PRESS or PRESS-ratio. The main focus here is to find the criterion that best approximates the response typically encountered in crashworthiness simulations. Based on a suite of analytical examples and crashworthiness simulation problems, it was concluded that the PRESS-based selection criterion performs the best and offers the least variation with the choice of experimental design, sampling density, and the nature of the problem.

I. Introduction

Most engineering problems of practical significance are computationally expensive. This phenomenon is common in crashworthiness optimization due to the high cost of the finite element simulations. To alleviate high computational cost, the use of meta-models has become increasingly popular. In this approach, meta-models are developed using the limited data and optimization is carried out using these computationally inexpensive surrogate models. There are many types of meta-models available in literature with polynomial response surfaces being the most popular due to their simplicity. Radial basis function networks (RBFs) have been gaining popularity for approximation because of their ability to model highly non-linear responses with low fitting cost.

Numerous instances have been reported of the use of radial basis functions in engineering applications. A small representative sample of some engineering applications is given as follows. Kurdila and Peterson [1], Li et al., [2] and Young et al. [3] used radial basis functions to approximate control conditions of nonlinear systems applied to aircraft and rockets. Wheeler et al. [4] used radial basis functions to model high pressure oxidizer discharge temperature for a space shuttle main engine. Papila et al. [5], Shyy et al. [6], Karakasis and Giannakoglou [7] used radial basis functions to design turbo-machinery and propulsion components. Meckesheimer et al. [8] used radial basis functions to approximate discrete/continuous responses in the design of a desk lamp. Rocha et al. [9] found RBFs to perform the best to approximate wing weight of subsonic transport vehicle. Zhang et al. [22] used radial basis functions to optimize a microelectronic packaging system. Reddy and Ganguli [11] used radial basis functions to assess structural damage in helicopter rotor blades. Glaz et al. [12] used RBFs to approximate vibration loads while designing the helicopter rotor blades. Panda et al. [13] used RBFs to predict flank wear in drills. Lanzi et al. [14] used RBFs to approximate crash capabilities of composite absorbers. Fang et al. [15] found that RBFs approximate different responses in crashworthiness simulations very well.

Though RBFs have been gaining popularity, the quality of approximation depends heavily on the topology of the network i.e., the number of radial basis functions, location of centers of neurons, radius of influence. Orr [16-20] and the references within discusses different issues in the selection of the number and location of centers and the radius of influence of neurons. To date, there is no consensus on the best

[1] Scientist, 7374 Las Positas Road, Livermore CA, Member AIAA
[2] Senior Scientist, 7374 Las Positas Road, Livermore CA, Member AIAA

method of selecting network topology though it is agreed that network topology has a large bearing on the output.

While generalized cross-validation error (also known as PRESS) has been demonstrated for selecting neural network topology [21-25], radial basis function network typically minimizes the root mean square error criterion [16-20, 26]. The influence of different criteria on the selection of RBF network topology is studied in this paper. Specifically, the most popular PRESS error criterion is compared with other criteria like root mean square error, and integrated pointwise ratio of generalization error that is defined as PRESS-ratio in a subsequent Section. A few analytical test examples and engineering application problems from crashworthiness simulations are used to compare the different methods.

The paper is arranged as follows. The theoretical model and stepwise procedure of RBF model construction is described in the next section. Test problems used to validate the proposed approach and performance metrics to appraise different criteria are described in Section 3. Test procedure and numerical setup for each example are detailed in Section 4. Results obtained for different examples are given in Section 5. Finally, the main conclusions are derived from this study are summarized in Section 6.

II. Radial Basis Function Theoretical Model

A response function $f(\mathbf{x})$ is approximated using a metamodel of the response $\hat{f}(\mathbf{x})$ as,

$$f(\mathbf{x}) = \hat{f}(\mathbf{x}) + \varepsilon, \tag{1}$$

where ε is the error in approximation.

A. Regression Problem

Radial basis functions (RBFs) were introduced as approximation functions by Hardy [27] in 1971 for approximation of the topographical data. This is a non-parametric approximation technique because no global form of the approximation function is assumed *a priori*. Instead, the approximation $\hat{f}(\mathbf{x})$ is represented as a linear combination of N_{RBF} radially symmetric functions (radial basis functions) $h(\mathbf{x})$ as,

$$\hat{f}(\mathbf{x}) = w_0 + \sum_{i=1}^{N_{RBF}} w_i h_i(\mathbf{x}), \tag{2}$$

where w_i is the weight associated with the i^{th} radial basis function.

While many monotonically radially varying functions have been used as RBFs, the Gaussian function is the most commonly used radial basis function. A typical Gaussian function is given as follows

$$h(\mathbf{x}) = \exp(-\|\mathbf{x}-\mathbf{c}\|^2 / \delta^2) = \exp(-(r/\delta_c)^2); \quad \delta_c = s \times r_c, \tag{3}$$

where **c** is the center of the radial basis function, r_c is the radius of the (radial basis function) neuron, and s is a spread constant. The behavior of a Gaussian function is shown in Figure 1. This is a radially decaying function i.e., the function value decays with increase in distance from the center. The Gaussian function assumes its peak value at the center and gradually decays to zero as $r \to \infty$. The rate of decay is controlled by δ_c, often known as the radius of influence. If the radius of influence is large, the rate of decay is slow; and if the radius of influence is small, the rate of decay of the function is high.

Typically, a radial basis function approximation is a two-level optimization. Firstly, one needs to determine the topology of the network i.e., the number of radial basis functions, corresponding center locations, radii, and spread constant. Subsequently, the weights associated with each RBF are estimated. Mostly, weights are estimated by minimizing a quadratic loss function L that is the sum of the square of errors of the approximation.

$$L(\mathbf{w}) = \sum_{i=1}^{N_{pts}} (f(\mathbf{x}^{(i)}) - \hat{f}(\mathbf{x}^{(i)}))^2. \quad (4)$$

This choice of the quadratic loss function allows the use of linear regression to estimate the weights vector. However, this may lead to overfitting of the data and may result in very large weights. Mullur and Messac [26] proposed the use of an extended RBF to avoid overfitting. However, a more conventional approach is to add a weight penalty to the loss function (Tikhonov and Arsenin, [28]),

$$L(\mathbf{w}) = \sum_{i=1}^{N_{pts}} (f(\mathbf{x}^{(i)}) - \hat{f}(\mathbf{x}^{(i)}))^2 + \sum_{i=0}^{N_{RBF}} \lambda_i w_i^2; \quad \lambda_i \geq 0, \quad (5)$$

where λ_i is the regularization parameter associated with the i^{th} weight. This formulation attempts to find parsimonious networks, thus reducing the sensitivity of the network to small changes.

Using ridge regression [18] to solve Equation (5), weights are estimated analytically as,

$$\hat{\mathbf{w}} = (H^T H + \Lambda)^{-1} H^T \mathbf{f}, \quad (6)$$

where $\mathbf{f}$ is the vector of responses at design points, Λ is a diagonal matrix such that $\Lambda_{ii} = \lambda_i$, $i = 0,1,..., N_{RBF}$, and H is the design matrix constructed using the response of radial basis functions at design points such that

$$H_{i1} = 1, H_{ij+1} = h_j(\mathbf{x}^{(i)}), \quad i = 1,..., N_{pts}, j = 1,..., N_{RBF}.$$

The predicted response at any point is

$$\hat{f}(\mathbf{x}) = \hat{w}_0 + \sum_{i=1}^{N_{RBF}} \hat{w}_i h_i(\mathbf{x}). \quad (7)$$

It is obvious from the above description that the performance of the network depends on the choice of the regularization parameters. Large λ_i might result in a large deviation from the data and very small λ_i may lead to overfitting. To reduce computational complexity involved in finding optimal regularization parameters, often a single regularization parameter is used $\lambda_i = \lambda, i = 0,1,..., N_{RBF}$. The most common methods to select an optimal value for λ are based on generalized cross-validation [29, 30], or the expectation maximization method [20]. Nevertheless, the computational cost of determining optimal regularization parameters is high for even moderate size problems, and increases with the number of samples. So a computationally efficient iterative procedure is implemented to select a 'good' regularization parameter in this study [31].

B. Error Metrics for RBFs

The quality of above approximation is assessed by using different error metrics. The most common error metrics are described as follows.

1. Root mean square error (NoiseVar)

The approximation error at the design points is,

$$\mathbf{e} = \mathbf{f} - H\hat{\mathbf{w}} = \mathbf{f} - H(H^T H + \Lambda)^{-1} H^T \mathbf{f} = (I - H(H^T H + \Lambda)^{-1} H^T)\mathbf{f} = P\mathbf{f}. \quad (8)$$

where I is an identity matrix of size N_{pt} and $P = I - H(H^T H + \Lambda)^{-1} H^T$. P is known as the projection matrix. The root mean square error (also an estimate of square root of noise variance) [18] is,

$$\hat{\sigma} = \sqrt{(\mathbf{e}^T \mathbf{e}) / trace(P)}. \tag{9}$$

2. Predicted residual sum of squares (PRESS)

Leave-one-out cross-validation error or PRESS is another popular and effective error measure [32, 33]. To compute PRESS, the response is approximated using the data at N_{pt} - 1 points and this approximation is used to compute the actual error at the left out point. This procedure is repeated for all N_{pt} points by leaving out each point exactly once. The expression for PRESS is

$$PRESS = \sum_{i=1}^{N_{pt}} (e_i^{PRESS})^2 = \sum_{i=1}^{N_{pt}} (f(\mathbf{x}^{(i)}) - \hat{f}^{-i}(\mathbf{x}^{(i)}))^2, \tag{10}$$

where $\hat{f}^{-i}(\mathbf{x}^{(i)})$ is the predicted response at design point $\mathbf{x}^{(i)}$ which was not used to construct the approximation $\hat{f}^{-i}$. The need to fit many networks to estimate PRESS can be obviated by using the projection matrix [18] and the vector of cross-validation error is computed as follows.

$$\mathbf{e}^{PRESS} = (diag(P))^{-1} P\mathbf{f}. \tag{11}$$

The root mean square of the PRESS which is compared to other error measures is

$$\hat{\sigma}_{PRESS} = \sqrt{PRESS / N_{pt}}. \tag{12}$$

3. Mean pointwise cross-validation error ratio (PRESS-ratio)

While the leave-one-out cross-validation error is a good measure of actual error, it might be susceptible to the large magnitude of error values. To avoid contamination of prediction error, an error ratio based criterion is given as follows:

$$\hat{\sigma}_{ratio} = \frac{1}{N_{pts}} \sum_{i=1}^{N_{pts}} \left| f(\mathbf{x}^{(i)}) \Big/ \hat{f}^{-i}(\mathbf{x}^{(i)}) - 1 \right|. \tag{13}$$

This criterion scales the magnitude of the errors thus eliminating the influence of a few large errors on the predictions but assigns more importance to the errors in the prediction of small values.

C. RBF Network Topology Selection

As discussed earlier, RBF network selection is a two-level optimization. The theoretical model for the second step, that is, the selection of weights for a given topology is well developed but there is no computationally efficient method available for the optimal selection of network topology (first step). Consequently, a trial and error procedure is used to select the suitable RBF network topology and optimal weights are selected for the best topology.

A stepwise procedure to construct a radial basis function network that is adopted in LS-OPT® [31] is given as follows.

1. Sample design points
2. Evaluate responses at design points
3. Select the criterion to select network topology
4. Identify the number of neurons
    a. Determine the spread constant
        i. Determine the location of centers and corresponding radii [31]

ii. Estimate the best regularization parameter(s) using the chosen topology selection criterion
iii. Estimate different error measures

b. Repeat the loop over different spread constants

5. Estimate the best spread using the chosen topology selection criterion
6. Repeat the loop (Step 4) for different number of neurons
7. Select the network topology that results in the best performance over the chosen topology selection criterion.

There are three optimization steps in selection of the RBF network topology, i) estimation of the regularization parameter, ii) estimation of the spread constant, and iii) choice of the number of neurons. While the choice of selection criterion can be different at each step, a consistent choice is maintained here. A different criterion can be used as objective function of the optimization process, e.g., minimization of the root mean square error, PRESS error, or PRESS-ratio.

In this paper, the influence of the three above-mentioned error criteria on the selection of network topology is studied. To isolate the influence of the error criterion on the prediction performance, the location of centers and radii is fixed across all networks for the chosen experimental design [31]. For the sake of simplicity, a single regularization parameter is used for all weights $\lambda_i = \lambda, \forall i$.

III. Test Problems and Performance Metrics

The performance of different RBF networks obtained by using different topology selection criteria is studied using a suite of analytical and crashworthiness test problems on a few error metrics. These examples and relevant error metrics are given as follows.

A. Test Problems

Two types of test problems are used in this study,

1. Analytical examples
2. Engineering problems from crashworthiness simulations

1. Branin-Hoo function [35]

$$f(x_1, x_2) = 10 + 10\left(1 - \frac{1}{8\pi}\right)\cos(x_1) + \left(x_2 - \frac{5.1}{4\pi^2}x_1^2 + \frac{5.0}{\pi}x_1 - 6\right), \tag{15}$$
$$-5 \le x_1 \le 10, \;\; 0 \le x_2 \le 15.$$

2. Camelback function [35]

$$f(x_1, x_2) = \left(\frac{x_1^4}{3} - 2.1x_1^2 + 4\right)x_1^2 + x_1x_2 + \left(4x_2^2 - 4\right)x_2^2, \tag{16}$$
$$-3 \le x_1 \le 3, \;\; -2 \le x_2 \le 2.$$

3. Goldstein-Price [35]

$$f(x_1, x_2) = \left[1 + (x_1 + x_2 + 1)^2(19 - 4x_1 + 3x_1^2 - 14x_2 + 6x_1x_2 + 3x_2^2)\right]$$
$$\times\left[30 + (2x_1 - 3x_2)^2(18 - 32x_1 + 12x_1^2 + 48x_2 - 36x_1x_2 + 27x_2^2)\right], \tag{17}$$
$$-2 \le x_1 \le 2, \;\; -2 \le x_2 \le 2.$$

4. Hartman [35]

$$f(\mathbf{x}) = -\sum_{i=1}^{4} c_i \exp\left(-\sum_{j=1}^{N_v} a_{ij}(x_j - p_{ij})^2 \right), \qquad (18)$$
$$0 \le x_j \le 1,\ j = 1, N_v.$$

1. Three variables: $N_v = 3$, The parameters are given in Table 1.
2. Six variables: $N_v = 6$, The parameters are given in Table 2. For this example, all variables were allowed to vary between 0 and 0.5.

5. Jin et al. [36] – two variables JIN2

$$f(x_1, x_2) = \left(30 + x_1 \sin(x_1)\right)\left(4 + \exp(-x_2^2)\right), \qquad (19)$$
$$0 \le x_1 \le 10,\ \ 0 \le x_2 \le 6.$$

6. Jin et al. [36] – ten variables J10a

$$f(\mathbf{x}) = \sum_{j=1}^{10} \exp(x_j)\left(t_j + x_j - \ln\left(\sum_{i=1}^{10} \exp(x_i) \right) \right), \qquad (20)$$
$$0.5 \le x_i \le 1, j = 1, N_{\mathrm{v}}.$$

The parameters used in this function are given in Table 3. This problem is not really non-linear.

7. Giunta and Watson [37]

$$f(\mathbf{x}) = \sum_{j=1}^{10} \left(0.3 + \sin\left(\frac{16}{15} x_j - 1 \right) + \sin^2\left(\frac{16}{15} x_j - 1 \right) \right),$$
$$-1 \le x_i \le 1, j = 1, N_v; \quad when\ \ N_v = 5, \qquad (21)$$
$$0 \le x_i \le 1, j = 1, N_v; \quad when\ \ N_v = 10.$$

This problem is studied for two instances of five and ten variables.

8. Multi-disciplinary analysis of a NHTSA vehicle undergoing full-frontal crash

Next, a multi-objective optimization problem of the crashworthiness simulation of a National Highway Transportation and Safety Association (NHTSA) vehicle undergoing full-frontal impact was analyzed. The goal of the optimization was to simultaneously reduce mass and intrusion, while satisfying the constraints on the torsional frequency, maximum intrusion, and different stage pulses [38]. For this multi-disciplinary analysis, the finite element model, containing approximately 30000 elements, was obtained from the National Crash Analysis Center (NCAC website) [39]. A modal analysis of the vehicle was conducted on the so-called 'body-in-white' model with approximately 18000 elements. The crash and vibration finite element models are shown in Figure 2 and the crash is simulated for 90ms.

The design variables were the gauges of different structural members that were affected. These members included aprons, outer and inner rails, inner and outer shotguns, cradle rail, and cradle cross-members (Figure 3). The description and ranges of these seven design variables is given in Table 4. The mathematical formulation of the optimization problem is as follows:

Minimize

Mass

Intrusion (x_{crash})

Subject to:

Maximum intrusion <= 551.27 mm

Stage 1 pulse >= 14.512g

Stage 2 pulse >= 17.586g

Stage 3 pulse >= 20.745g

41.385 Hz <= Torsional mode frequency <= 42.38 Hz

The stage pulses are calculated from the SAE filtered (60 Hz) acceleration $\ddot{x}$ and displacement x of a left rear sill node as

$$Stage\,i\ pulse = -k\left(\int_{d_1}^{d_2} \ddot{x}dx \Big/ \int_{d_1}^{d_2} dx\right), \tag{22}$$

where k=0.5 for $i=1$, otherwise k=1. The minus sign was used to convert acceleration to deceleration. The limits on the integration for different stage pulse were (0:184) for $i=1$, (184:334) for $i=2$, and (334: maximum displacement) for $i=3$. LS-DYNA® [40] was used to simulate different designs. It took approximately 50 minutes to run a single crashworthiness simulation on a dual-core Intel Xeon (2.66 GHz) processor with 4 GB memory.

9. Automotive instrument panel structure (Knee-impact) simulation

The second crashworthiness example employs a finite element simulation of a typical automotive instrument panel (shown in Figure 4) impacting the knees [41]. The spherical object that represents knee moves in the direction determined from prior physical tests. The instrument panel (IP) comprises of a knee bolster that also serves as a steering column cover with a styled surface, and two energy absorption brackets attached to the cross vehicle IP structure. A significant portion of the lower torso energy of the occupant is absorbed by appropriate deformation of these brackets. The wrap-around of the knee around the steering column is delayed by adding a device, known as the yoke, to the knee bolster system. The shape of the brackets and yoke are optimized without interfering with the styled elements. The eleven design variables are shown in Figure 5 and the ranges are given in Table 5. To keep the computational expense low, only the driver side instrument panel was modeled using 25000 elements and the crash was simulated for 40ms, by which time the knees have been brought to rest. The design optimization problem accounting for the optimal occupant kinematics is formulated as follows:

Minimize

Mass

Subject to:

Left knee force <= 3250

Right knee force <= 3250

Left knee displacement <= 115

Right knee displacement <= 115

Yoke displacement <= 85

Kinetic energy <= 154000

All responses are scaled. Knee forces are the peak SAE filtered (60 Hz) forces whereas all the displacements are represented by the maximum intrusion. LS-DYNA [40] was used to simulate the different designs. Each simulation requires approximately 60 minutes on a dual-core Intel Xeon (2.66 GHz) processor with 4 GB memory.

10. Head-impact analysis

Finally, the impact of an occupant head form against an A-pillar of a vehicle was analyzed. An interior trim cover with interior ribs was provided to soften the impact (Figure 6). The design was required to minimize a head injury criterion (HIC-d) that was obtained from the head injury coefficient obtained at 15ms (HIC).

The design variables for this example are given in Table 6. A single analysis was completed in approximately 20 minutes on a dual-core Intel Xeon (2.66 GHz) processor with 4 GB memory.

B. Performance Metrics

The performance of the predictions is compared using the following three metrics

1. Correlation between predicted and observed responses

The correlation coefficient is calculated as

$$R(f,\hat{f}) = \frac{1}{V\left(\sigma(f)\sigma(\hat{f})\right)}\int_V (f-\bar{f})(\hat{f}-\bar{\hat{f}})dV, \tag{23}$$

where $\bar{f}$ and $\sigma(f)$ are the mean and standard deviation of actual responses, $\bar{\hat{f}}$ and $\sigma(\hat{f})$ are the mean and standard deviation of the predicted responses, and V is the volume of the domain. The mean and standard deviations are computed as

$$\bar{f} = \frac{1}{V}\int_V f dV;\ \ \sigma(f) = \sqrt{\frac{1}{V}\int_V (f-\bar{f})^2 dV}. \tag{24}$$

A high correlation coefficient is desired for a good quality of approximation.

The above equations are numerically evaluated using the data at test points by implementing quadrature for integration [42] as follows.

$$\bar{f} = \sum_{i=1}^{N_{test}} \gamma_i f_i \Big/ \sum_{i=1}^{N_{test}} \gamma_i \,.\ \sigma(f) = \sqrt{\sum_{i=1}^{N_{test}} \gamma_i (f_i-\bar{f})^2 \Big/ \sum_{i=1}^{N_{test}} \gamma_i}\,. \tag{25}$$

$$\frac{1}{V}\int_V f\hat{f} dV = \sum_{i=1}^{N_{test}} \gamma_i f_i \hat{f}_i \Big/ \sum_{i=1}^{N_{test}} \gamma_i\,. \tag{26}$$

In the above equations, γ_i represents the weight associated with the i^{th} test point, as determined by the quadrature for integration. For uniform grid of points, the Simpson's integration rule is used whereas for non-uniform grids, the Monte Carlo integration method is used.

The correlation coefficient captures the prediction trends but yields no information about the actual errors of approximation, which can be high despite a high correlation. So the approximation errors are quantified using two error-based criteria.

2. Root mean square error in the predictions

The root mean square error at the test points is given as

$$RMSE = \sqrt{\frac{1}{V}\int_V (f-\hat{f})^2 dV}\,. \tag{27}$$

Using the quadrature, the RMSE is estimated as

$$RMSE = \sqrt{\sum_{i=1}^{N_{test}} \gamma_i (f_i-\hat{f}_i)^2 \Big/ \sum_{i=1}^{N_{test}} \gamma_i}\,. \tag{28}$$

3. Maximum absolute error in the predictions

Another measure of the quality of any approximation is the maximum absolute error:

$$MaxE = \max_i \left| f_i - \hat{f}_i \right|. \tag{29}$$

A good approximation yields low errors and high correlation.

IV. Test Procedure and Numerical Setup

A. Test Procedure

For each test example, the stepwise test procedure to identify the best topology selection criterion is outlined as follows:

1. Identify an experimental design.
2. Conduct function evaluations at the design points.
3. Identify the different RBF network topologies using the following criteria,
   a. Minimize the square root of the error in prediction
   b. Minimize the root mean square of the PRESS error
   c. Minimize the mean PRESS-ratio.
4. For each RBF network, estimate the predicted responses and errors at the test points.
5. For each network, compute the test metrics.
6. Repeat the procedure starting from Step 1, 1000 times for each example to minimize the influence of randomness in experimental designs.
7. Summarize the results using mean and coefficient of variation of test metrics.

B. Numerical Setup

The numerical setup used to analyze the different examples is summarized in Table 7. The number of sampling points was taken such that a reasonable approximation of the underlying function could be obtained. For all the analytical examples, the experimental designs were selected in two steps. Firstly, a large set with N_{LHS} points was generated using a Latin hypercube sampling (LHS)[3] criterion. This set was used as the basis set to select N_S points using the D-optimality criterion[4] [43]. 1000 such experimental designs were used to minimize the sensitivity of the results due to the random selection of experimental designs. To compare different approximations, N_{test} independent test points, selected using the Latin hypercube sampling criterion, were used.

For the multi-disciplinary crashworthiness example, 4800+ designs were analyzed during a multi-objective optimization using a genetic algorithm [44]. This data set was used as a basis set to select N_S experimental designs randomly. 1000 experimental designs were used to study the influence of the experimental designs. All the points were used as test points. For the instrument panel knee-impact simulation, the data for a total of 851 unique simulations was available. This set was used to randomly select experimental designs and test points. Similarly, for the head impact analysis, the experimental designs and test points were selected from a pool of 1289 unique points.

V. Results

In this section, the results of comparison of the different criteria for network selection are summarized. Results for analytical examples and crashworthiness simulations are summarized in Figure 7–Figure 12.

A. Correlation Coefficient

The correlation between actual and predicted responses using different RBF networks for analytical examples and responses of crashworthiness simulations are shown in Figure 7–Figure 10 (A/B). The mean values and coefficient of variation were estimated using 1000 experimental designs. It was observed that no single criterion performed the best for all examples. The network topologies selected using the RMS error (*NoiseVar*) based criterion performed well in predicting the analytical functions and responses from the head-impact analysis and knee-impact analysis, however, the performance in approximating the responses

[3] The Matlab® routine 'lhsdesign' with 'maximin' criterion that maximizes the minimum distance between points is used to generate LHS designs. 500 iterations were used to find an optimum design.

[4] The order of the polynomial to estimate D-optimality is chosen such that the number of points is approximately twice the number of coefficients. Duplicate points were not allowed. The Matlab® routine 'candexch' with a maximum of 100 iterations were used to find the optimal experimental design.

for multi-disciplinary crash simulation was very poor. Also, as depicted by the high coefficient of variation, the RMS error (*NoiseVar*) based criterion showed high sensitivity to the choice of experimental design.

The RBF networks selected using the PRESS-ratio based criterion performed well for most problems though it showed large variability with the choice of experimental design for analytical examples. On the other hand, the PRESS-based topology selection criterion showed robust performance in approximating all analytical and crashworthiness examples. This criterion also resulted in the least variability with the choice of experimental designs. For most responses, the PRESS-based criterion outperformed the PRESS-ratio based criterion. The influence of dimensionality was not significant as all RBF topology selection criteria showed similar trends.

B. Root Mean Square Error

The mean and coefficient of variation of root mean squared error at test points based on 1000 experimental designs obtained for different problems are shown in Figure 7–Figure 10 (C/D). It was observed that the RMS error (*NoiseVar*) based criterion typically yielded high mean root mean squared errors at the test points. Besides, the high coefficient of variation for the RMS error based criterion suggested high sensitivity to the choice of experimental design for both the analytical examples and the crashworthiness simulation responses. The PRESS-ratio based criterion performed better than the RMS error (*NoiseVar*) based criterion but in general this criterion was inferior to the PRESS-based selection criterion. The PRESS-based criterion provided the lowest root mean squared errors in approximation and a low coefficient of variation. It is interesting to note that for the head-impact analysis, while the RMS error (*NoiseVar*) based criterion resulted in the best correlation, the errors in approximation using this network were the highest.

C. Maximum Absolute Error

The results obtained for root mean square approximation errors were also valid for the maximum absolute error test metric.

It can be concluded that the PRESS criterion to select network topology yielded robust and the best performance for all analytical and crashworthiness simulation responses. Other criteria (PRESS-ratio and RMS error based criteria) performed well for selected responses only and were more susceptible to the nature of the underlying response and the choice of experimental designs.

D. Influence of sampling density

Since crashworthiness computations are expensive, most approximations are carried out using data from a few simulations. It is important to compare the three RBF topology selection criteria for a small number of data points.

The analytical example GW5 was approximated with 42 points and predictions were carried out at the same set of test points. The mean and coefficient of variation of correlation, RMS error and maximum absolute errors based on 1000 experimental designs were compared with the approximations based on 100 points in Table 8. As expected, low point density resulted in higher RMS and maximum errors, and lower correlation compared to the approximation based on 100 points. Nevertheless, the PRESS-based criterion performed significantly better (higher correlation, lower errors, lower coefficient of variations) than the PRESS-ratio based criterion and RMS error (*NoiseVar*) based criterion among all RBF networks constructed using the same number of design points.

To assess the influence of low sampling density on crashworthiness simulations, the multi-disciplinary crashworthiness example was approximated with 100 points and the IP structure knee impact problem was modeled using 50 points. The correlation, RMS, and maximum errors for the two examples with reduced sampling density are shown in Figure 11 and Figure 12, respectively. Comparing the MDO crashworthiness example results from Figure 8 (250 points experimental design) and Figure 11 (100 points experimental design), and the knee-impact example results from Figure 9 (100 points experimental design) and Figure 12 (50 points experimental design), it can be concluded that the PRESS based criterion was the best and the RMS error (*NoiseVar*) based criterion was the worst even when a smaller number of points was available. As expected, the approximations based on higher sampling density were better (higher correlation, lower errors, lower coefficient of variations) when the network topologies were selected using PRESS/PRESS-ratio based criteria. However, the quality of the approximations deteriorated with sampling density when the RMS error (*NoiseVar*) criterion was used to optimize RBF topology. This result indicates the danger of over-fitting by using the RMS error based criterion.

VI. Conclusions

In this study, three criteria to select optimal RBF network topology for crashworthiness response approximation were compared using a number of analytical and crashworthiness simulation problems ranging from two to eleven variables. The influence of sampling density and choice of experimental designs were assessed simultaneously. The results indicated that the choice of best network topology selection criterion depends on the problem and experimental design. However, the PRESS-based criterion to select RBF network topology resulted in the robust performance for all examples, experimental designs, and sampling densities. The PRESS-ratio based selection criterion also performed reasonably well, but it had high sensitivity to the choice of experimental design for the analytical examples. Often the network selected using the PRESS criterion, outperformed the network selected using the PRESS-ratio based criterion. It was observed that the RMS error (*NoiseVar*) based criterion was the worst of the three criteria for crashworthiness response approximation. The performance of the RMS error based criterion was very sensitive to the choice of experimental design and sampling density. Also with the increase in the number of points used for approximation, the RMS error selection criterion resulted in networks that over-fitted the data. In summary, the PRESS-based selection criterion is recommended for the selection of network topologies. This criterion has therefore been chosen as the default criterion for RBF topology selection in LS-OPT®.

VII. References

1. Kurdila AJ, Peterson JL, "Adaptation of Centers of Approximation for Nonlinear Tracking Control", *Journal of Guidance Control, and Dynamics,* **19**(2), 1996, pp. 363-369.
2. Li Y, Sundarajan N, Saratchandran P, "Stable Neuro-Flight Controller Using Fully Tuned Radial Basis Function Neural Networks", *Journal of Guidance, Control and Dynamics*, **24**(4), 2001.
3. Young A, Cao C, Patel V, Hovakimyan N, Lavertsky E, "Adaptive Control Design Methodology for Nonlinear-in-Control Systems in Aircraft Application", *Journal of Guidance, Control and Dynamics*, **30**(6), 2007.
4. Wheeler KR, Dhawan AP, Meyer CM, "Space Shuttle Main Engine Sensor Modeling using Radial Basis Function Neural Networks", *Journal of Spacecraft and Rockets*, **31**(6), 1994, pp. 1054-1060.
5. Papila N, Shyy W, Griffin L, Dorney DJ, "Shape Optimization of Supersonic Turbines using Global Approximation Methods", *Journal of Propulsion and Power*, **18**(3), 2002, pp. 509-518.
6. Shyy W, Papila N, Vaidyanathan R, Tucker K, "Global Design Optimization for Aerodynamics and Rocket Propulsion Components", *Progress in Aerospace Sciences*, **37**(1), 2001, pp. 59-118.
7. Karakasis MK, Giannakoglou KC, "On the use of Metamodel Assisted Multi-objective Evolutionary Algorithms", *Engineering Optimization*, **38**(8), 2006, pp. 941-957.
8. Meckesheimer M, Barton RR, Simpson T, Limayen F, Yannou B, "Metamodeling of Discrete/Continuous Responses", *AIAA Journal*, **39**(10), 2001, pp. 1950-1959.
9. Rocha H, Li W, Hahn A, "Principal Component Regression for Fitting Wing Weight Data of Subsonic Transports", *Journal of Aircraft*, **43**(6), 2006, pp. 1925-1936.
10. Zhang T, Choi KK, Rahman S, Cho K, Baker P, Shakil M, Heitkamp D, "A Hybrid Surrogate and Pattern Search Optimization Method and Application to Microelectronics", *Structural and Multi-disciplinary Optimization*, **32**(4), 2006, pp. 327-345.
11. Reddy RRK, Ganguli R, "Structural Damage Detection in a Helicopter Rotor Blade using Radial Basis Function Neural Networks", *Smart Materials and Structures*, **12**, 2003, pp. 232-241.
12. Glaz B, Friedmann PP, Liu L, "Surrogate based Optimization of Helicopter Rotor Blades for Vibration Reduction in Forward Flight", *Structural and Multi-disciplinary Optimization*, in press.
13. Panda SS, Chakraborty D, Pal SK, "Flank Wear Prediction in Drilling using Back Propagation Neural Networks and Radial Basis Function Network", *Applied Soft Computing*, 2007, in press.
14. Lanzi L, Castelletti LML, Anghileri M, "Multi-objective Optimization of Composite Absorber Shape under Crashworthiness Requirements", *Composite Structures*, **65**(3-4), 2004, pp. 433-441.
15. Fang H, Rais-Rohani M, Liu A, Horstemeyer MF, "A Comparative Study of MetaModeling Methods for Multi-objective Crashworthiness Optimization", *Computers and Structures*, **83**(25-26), 2005, pp. 2121-2136.
16. Orr MJL, "Local Smoothing of Radial Basis Function Networks", *Center for Cognitive Science*, University of Edinburgh, 1995.

17. Orr MJL, "Regularization in the Selection of Radial Basis Function Centers", *Center for Cognitive Science*, University of Edinburgh, 1995.
18. Orr MJL, "Introduction to Radial Basis Function Networks", *Center for Cognitive Science*, University of Edinburgh, 1996.
19. Orr MJL, "Optimizing the Widths of Radial Basis Functions", *Center for Cognitive Science*, University of Edinburgh, 1998.
20. Orr MJL, "Recent Advances in Radial Basis Function Networks", *Institute of Adaptive and Neural Computation*, University of Edinburgh, 1999.
21. Utans J, Moody J, "Selecting Neural Network Architecture via the Prediction Risk: Application to Corporate Bond Rating Prediction", In *Proceedings of the First International Conference on Artificial Intelligence Applications on Wall Street*, IEEE Computer Society Press, Los Alamitos CA, 1991.
22. Zhang P, "Model Selection via Multifold Cross Validation", *The Annals of Statistics*, **21**(1), 1993, pp. 299-313.
23. Moody J, Utans J, "Architecture Selection Strategies for Neural Networks: Application to Corporate Bond Rating Prediction", *Neural Networks in the Capital Markets* (editor A. N. Refenes), Wiley, 1994.
24. Anderson T, Martinez T, "Cross validation and MLP Architecture Selection", *Neural Networks*, **3**, 1999, pp. 1614-1619.
25. Vasios CE, Matsopoulos GK, Ventouras EM, Nikita KS, Uzunoglu N, "Cross-validation and Neural Network Architecture Selection for the Classification of Intracranial Current Sources", In *Proceedings of 7th Neural Network Applications in Electrical Engineering (NEUREL 2004)*, Belgrade, Sept 2004, pp. 151-185.
26. Mullur AA, Messac A, "Extended Radial Basis Functions: More Flexible and Effective Metamodeling", *AIAA Journal*, **43**(6), 2005, pp 1306-1315.
27. Hardy RL, "Multiquadrics Equations of Topography and Other Irregular Surfaces", *Journal of Geophysical Research*, **76**, 1991, pp. 1905-1915.
28. Tikhonov AN, Arsenin VY, *Solutions to Ill-posed Problems*, Wiley, New York, 1977.
29. Golub G, Heath M, Wahba G, "Generalized Cross-Validation as a Method for Choosing a Good Ridge Parameter", *Technometrics*, **21**(2), 1979, pp. 215-223.
30. Golub GH, von Matt U, "Generalized Cross-Validation for Large Scale Problems", *Journal of Computational and Graphical Statistics*, **6**(1), 1997, pp. 1-34.
31. Stander N, Roux W, Goel T, Eggleston T, Craig K, "LS-OPT Manual v 3.3", *Livermore Software Technology Corporation*, Livermore CA, 2007.
32. Goel T, Haftka RT, Shyy W, Queipo NV, "Ensemble of Surrogates", *Structural and Multidisciplinary Optimization*, **33**, 2007, pp. 199-216.
33. Goel T, Haftka RT, Shyy W, "Error Measures on Surrogate Approximation Based on Noise-free Data", In *Proceedings of 46th AIA Aerospace Sciences Meeting and Exhibit*, Reno NV, 2008, AIAA-2008-0901.
34. Deb K, *Multi-Objective Optimization Using Evolutionary Algorithms*, Wiley Chichester, 2001.
35. Dixon LCW, Szego GP, *Towards Global Optimization 2*, North Holland, Amsterdam, 1978.
36. Jin R, Chen W, Simpson T, "Comparative Studies of Metamodeling Techniques under Multiple Modeling Criteria", *Structural and Multidisciplinary Optimization*, **23**(1), 2001, pp. 385-398.
37. Giunta AA, Watson LT, "A Comparison of Approximation Modeling Techniques: Polynomial versus Interpolating Models", In *Proceedings of 7th AIAA/UAF/NASA/ISSMO Symposium on Multidisciplinary Analysis and Optimization*, St. Louis MO, 1998, AIAA-98-4758.
38. Craig KJ, Stander N, Dooge DA, Varadappa S, "Automotive Crashworthiness Design Using Response Surface-Based Variable Screening and Opimization", *Engineering Optimization*, **22**(1), 2005, pp. 38-61.
39. National Crash Analysis Center (NCAC), Public Finite Element Model Archive, www.ncac.gmu.edu/archives/model/index.html, 2001.
40. Livermore Software Technology Corporation, "LS-Dyna Manual v 971", Livermore CA, 2007.
41. Akkerman A, Thyagarajan R, Stander N, Burger M, Kuhm R, Rajic H, "Shape Optimization for Crashworthiness Design using Response Surfaces", Proceedings of the International Workshop on Multidisciplinary Design Optimization, Pretoria SA, 2000, pp. 270-279.

42. Ueberhuber CW, *Numerical Computation 2: Methods, Software, and Analysis*, Springer, New York, p 71.
43. Goel T, Haftka RT, Shyy W, Watson LT, "Pitfalls of Using a Single Criterion for Selecting Experimental Designs", *International Journal of Numerical Methods in Engineering*, **75**(2), 2008, pp. 127-155.
44. Li G, Goel T, Stander N, "Assessing the Convergence Properties of NSGA-II for Direct Crashworthiness Optimization", In Proceedings of the *10th International LS-DYNA Users Conference*, Detroit MI, Jun 8-10, 2008.

Table 1. Parameters in the Hartman problem with three design variables.

i	a_{ij}			c_i	p_{ij}		
1	3.0	10.0	30.0	1.0	0.3689	0.1170	0.2673
2	0.1	10.0	35.0	1.2	0.4699	0.4387	0.7470
3	3.0	10.0	30.0	3.0	0.1091	0.8732	0.5547
4	0.1	10.0	35.0	3.2	0.03815	0.5743	0.8828

Table 2. Parameters in the Hartman problem with six design variables.

i	a_{ij}						c_i
1	10.0	3.0	17.0	3.5	1.7	8.0	1.0
2	0.05	10.0	17.0	0.1	8.0	14.0	1.2
3	3.0	3.5	1.7	10.0	17.0	8.0	3.0
4	17.0	8.0	0.05	10.0	0.1	14.0	3.2
i	p_{ij}						
1	0.1312	0.1696	0.5569	0.0124	0.8283	0.5886	
2	0.2329	0.4135	0.8307	0.3736	0.1004	0.9991	
3	0.2348	0.1451	0.3522	0.2883	0.3047	0.6650	
4	0.4047	0.8828	0.8732	0.5743	0.1091	0.0381	

Table 3. Parameters used in the JIN-10 function.

	Value		Value
t_1	-6.089	t_6	-14.986
t_2	-17.164	t_7	-24.100
t_3	-34.054	t_8	-10.708
t_4	-5.914	t_9	-26.662
t_5	-24.721	t_{10}	-22.179

Table 4. Design variables used for the multi-disciplinary crashworthiness simulation of National Highway Transport and Safety Association (NHTSA) vehicle.

Variable name	Lower bound	Baseline design	Upper bound
Rail inner	1.0	2.0	3.0
Rail outer	1.0	1.5	3.0
Cradle rails	1.0	1.93	3.0
Aprons	1.0	1.3	2.5
Shotgun inner	1.0	1.3	2.5
Shotgun outer	1.0	1.3	2.5
Cradle cross member	1.0	1.93	3.0

Table 5. Design variables used for the simulation of automotive instrument panel structure (knee-impact) analysis.

Variable name	Lower bound	Baseline design	Upper bound
L-Bracket gauge	0.7	1.1	3.0
T-Flange depth	20.0	28.3	50.0
F-Flange depth	20.0	27.5	50.0
B-Flange depth	15.0	22.3	50.0
I-Flange width	5.0	7.0	25.0
L-Flange width	20.0	32.0	50.0
R-Bracket gauge	0.7	1.1	3.0
R-Flange width	20.0	32.0	50.0
R-Bracket radius	10.0	15.0	25.0
Bolster gauge	1.0	3.5	6.0
Yolk radius	2.0	4.0	8.0

Table 6. Design variables in head-impact analysis simulation.

Variable name	Lower bound	Baseline design	Upper bound
Trim thickness	2.0	2.0	3.5
Number of ribs	3	3	15
Rib thickness	0.8	1.0	2.0
Rib height	5.0	6.0	20.0
Span	130.0	180	180

Table 7. Numerical setup for different examples. N_v ***is the number of variables,*** N_{pts} ***is the number of samples used for approximation,*** N_{LHS} ***is the number of basis points used for the D-optimality criterion,*** N_{poly} ***is the order of polynomial used for estimating D-optimality, and*** N_{test} ***is the number of test points.***

Example	N_v	N_{pts}	N_{LHS}	N_{poly}	N_{test}
Branin-Hoo	2	20	100	3	150
Camelback	2	30	150	4	150
Goldstein-Price	2	42	200	5	150
Jin-2	2	30	150	4	150
Hartman-3	3	70	250	3	500
GW5	5	100	400	3	2000
Hartman-6	6	56	200	2	2000
Jin-10a	10	150	450	2	5000
GW10	10	150	450	2	5000
NHTSA[*]	7	250	4847	-	4847
Knee-impact[*]	11	100	851	-	851
Head-impact[*]	5	42	1289	-	1289

[*]Experimental points are selected randomly from all the data points.

Table 8. Influence of sampling density on the approximation of the GW5 example.

		PRESS		GCV-ratio		Noise Variance	
	# of points	Mean	COV	Mean	COV	Mean	COV
Correlation	42	0.336	(0.572)	0.324	(0.603)	0.317	(0.482)
	100	0.966	(0.014)	0.966	(0.013)	0.969	(0.011)
RMSE	42	0.207	(0.106)	0.220	(0.321)	0.262	(0.473)
	100	0.055	(0.178)	0.055	(0.176)	0.053	(0.166)
Max Error	42	0.698	(0.160)	0.796	(0.585)	1.155	(0.884)
	100	0.308	(0.337)	0.308	(0.335)	0.303	(0.335)

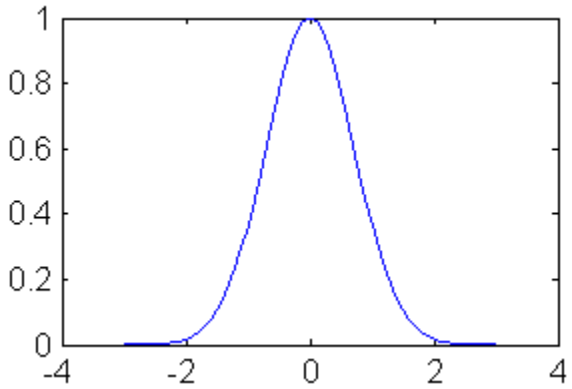

Figure 1. Gaussian radial basis function with center located at x=0.

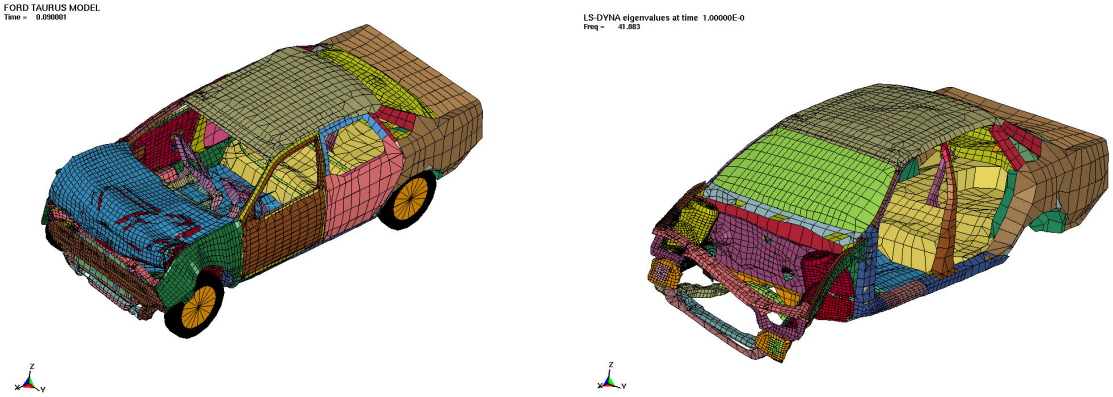

A) Crash simulation model B) Body-in-white model for NVH simulation

Figure 2. Finite element models of a National Highway Transport and Safety Association vehicle.

Figure 3. Exploded view of structural components in NHTSA vehicle influenced by design variables.

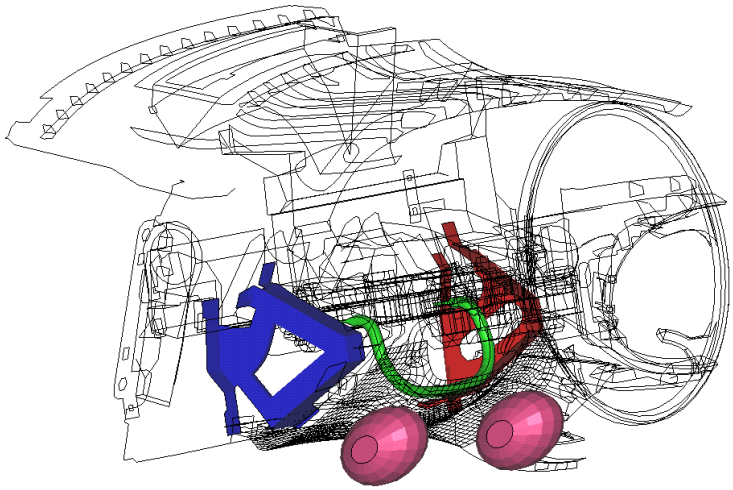

Figure 4. Automotive instrument panel with knee bolster system used for knee-impact analysis. (Courtesy: Ford Motor Company)

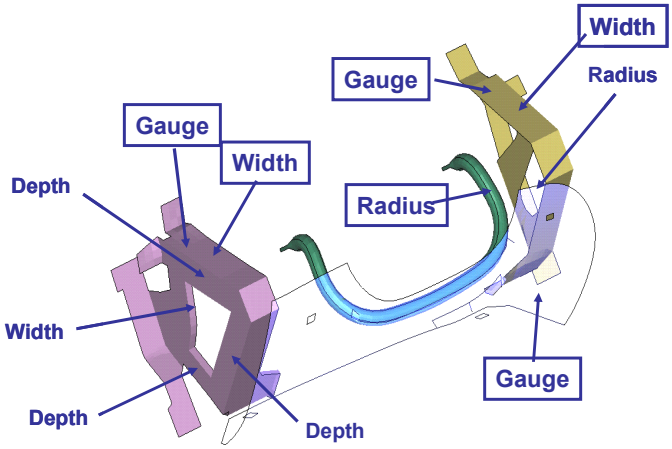

Figure 5. Design variables of the knee bolster system.

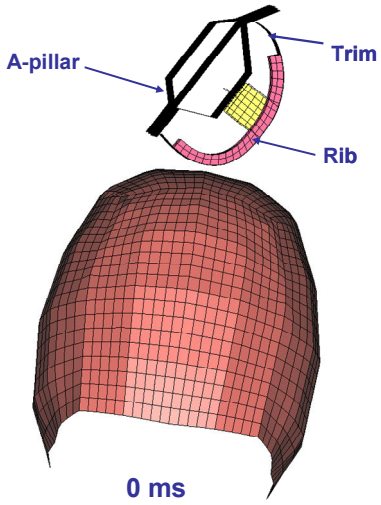

Figure 6. Head impact of A-pillar with trim

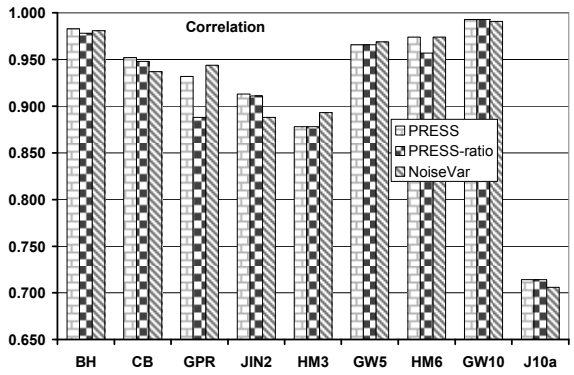

A) Mean – Correlation

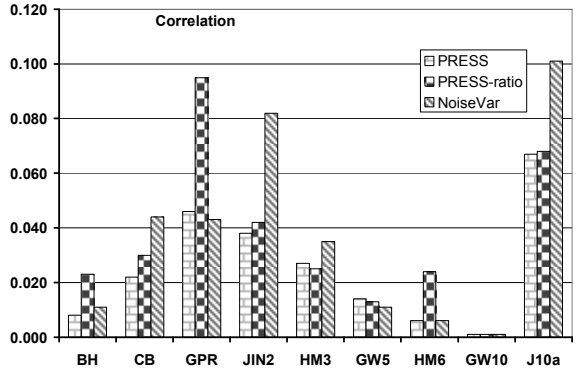

B) Coefficient of variation – Correlation

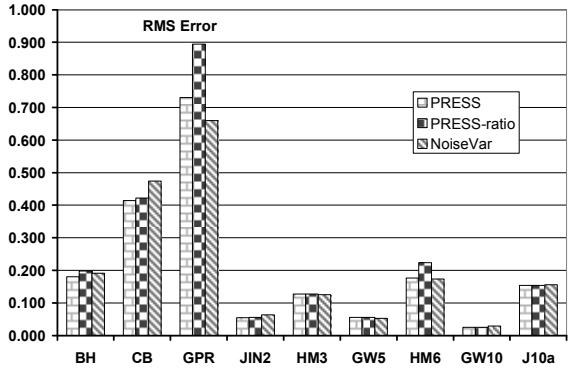

C) Mean – Root mean square error

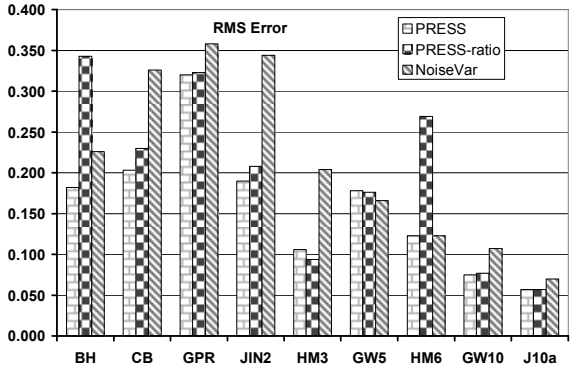

D) Coefficient of variation – RMSE

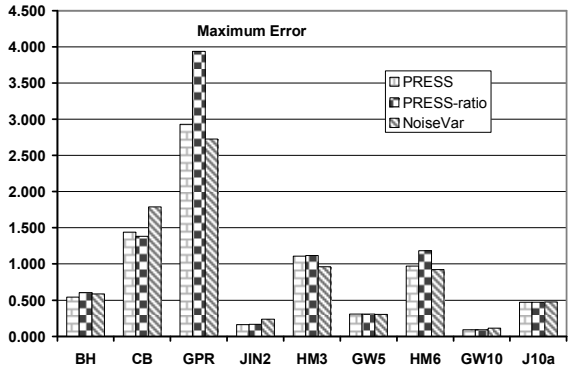

E) Mean – Maximum absolute error

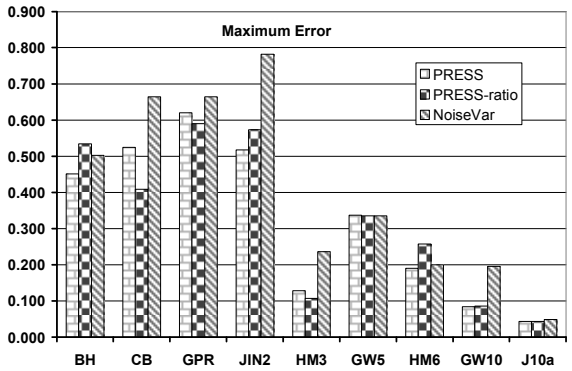

F) Coefficient of variation – Maximum absolute error

Figure 7. Analytical examples: Comparison of different RBF network topology selection criteria (PRESS: predicted residual sum of squares, PRESS-ratio: averaged pointwise ratio of PRESS errors, NoiseVar: RMS error) based on 1000 DOEs. BH – Branin-Hoo, CB – Camelback, GPR – Goldstein-Price, JIN2, J10a – Jin et al. problem with two and ten variables, HM3,6 – Hartman problem with three and six variables, GW5, 10 – Giunta-Watson problems with five and ten variables.

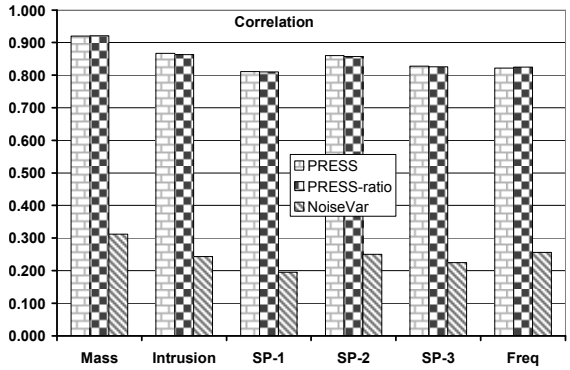

A) Mean – Correlation

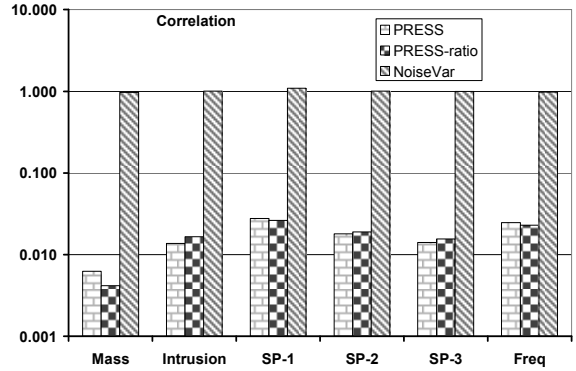

B) Coefficient of variation – Correlation

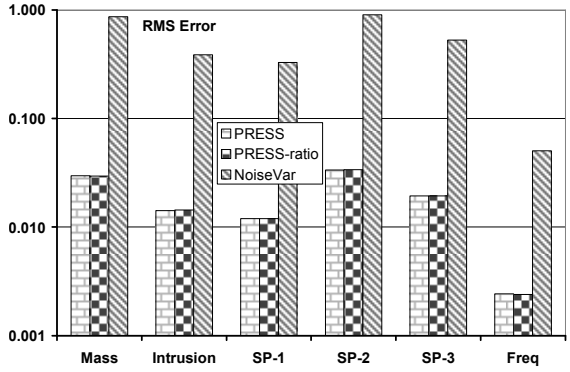

C) Mean – Root mean square error

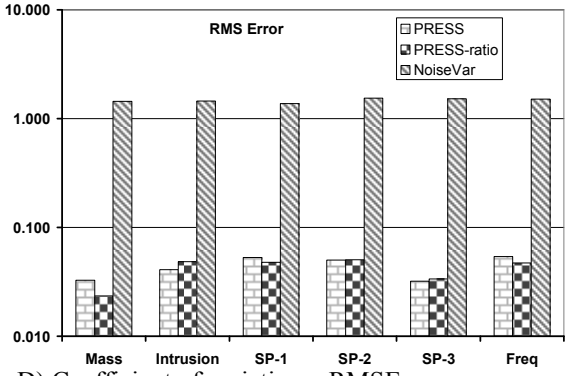

D) Coefficient of variation – RMSE

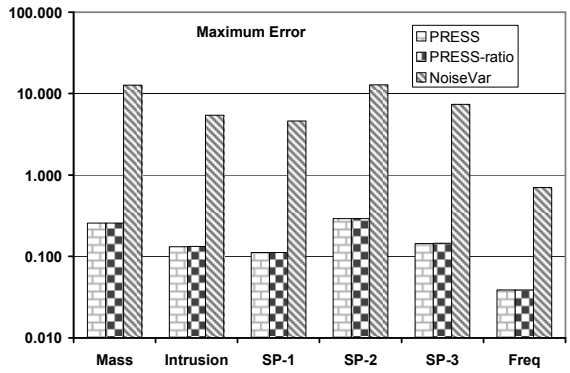

E) Mean – Maximum absolute error

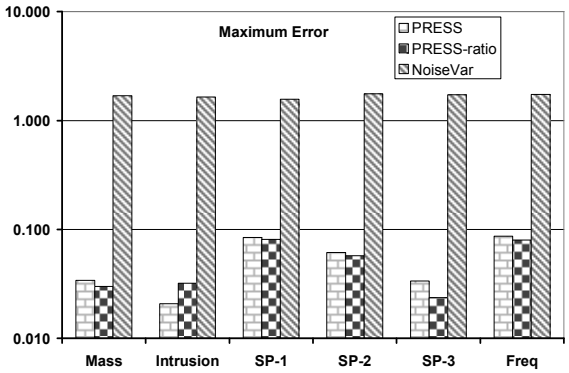

F) Coefficient of variation – Maximum absolute error

Figure 8. MDO crashworthiness example: Comparison of different RBF network topology selection criteria for approximation of responses in multi-disciplinary crashworthiness analysis (based on 250 points, 1000 DOEs). (PRESS: predicted residual sum of squares, PRESS-ratio: averaged pointwise ratio of PRESS errors, NoiseVar: RMS error) SP-1 indicates Stage 1 pulse, SP-2 is Stage 2 pulse and SP-3 is Stage 3 pulse.

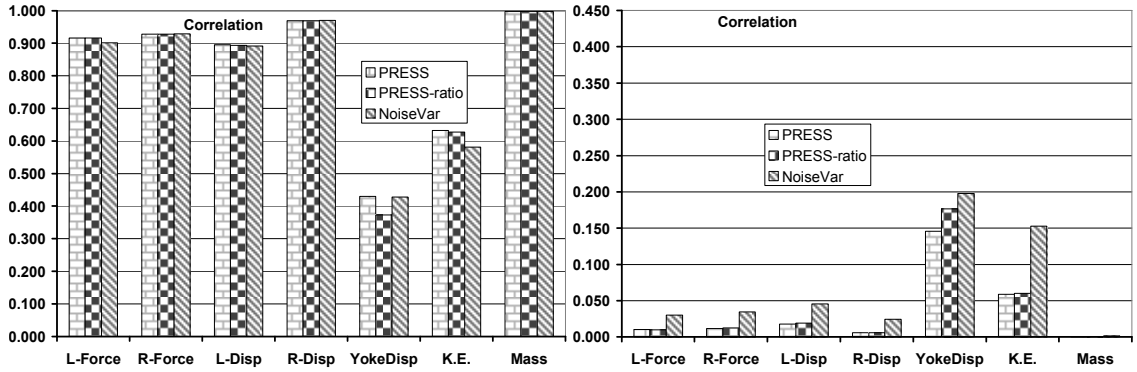

A) Mean – Correlation

B) Coefficient of variation – Correlation

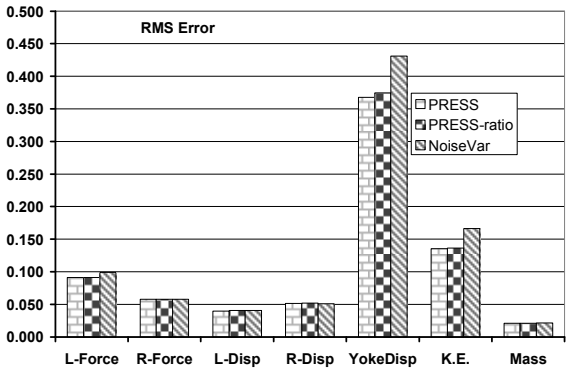

C) Mean – Root mean square error

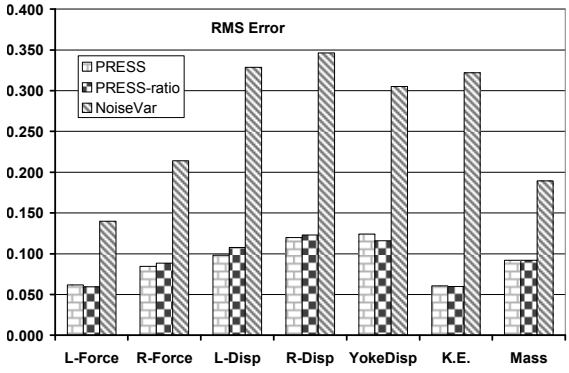

D) Coefficient of variation – RMSE

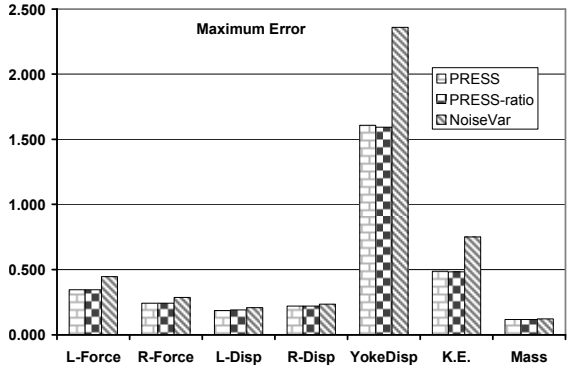

E) Mean – Maximum absolute error

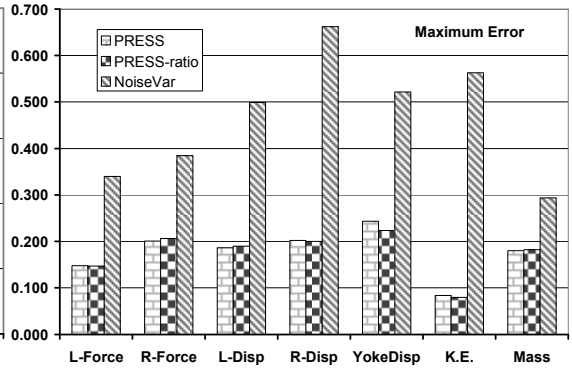

F) Coefficient of variation – Maximum absolute error

Figure 9. Instrument panel knee-impact analysis: Comparison of different RBF network topology selection criteria (PRESS: predicted residual sum of squares, PRESS-ratio: averaged pointwise ratio of PRESS errors, NoiseVar: RMS error) for approximation of responses in crashworthiness simulations of the automotive instrument panel structure knee impact analysis (based on 100 points, 1000 DOEs). K.E. – kinetic energy.

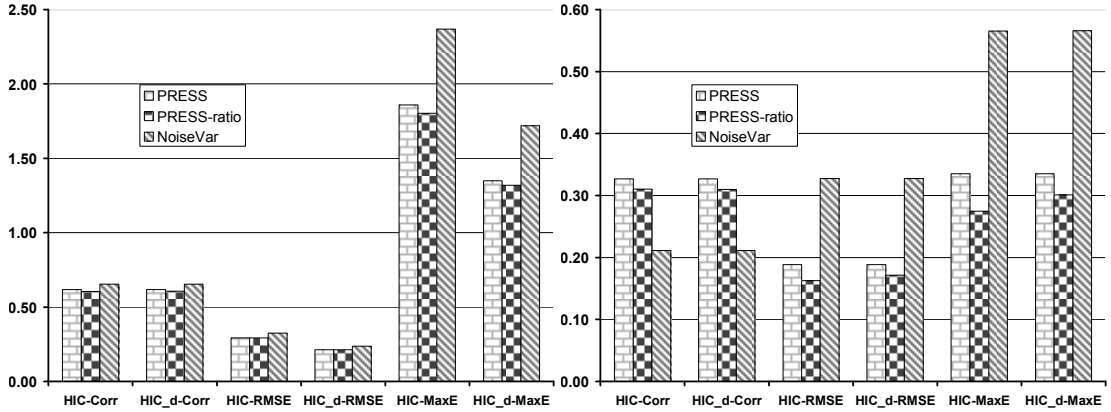

A) Mean B) Coefficient of variation

Figure 10. Head impact analysis: Comparison of different RBF network topology selection criteria (PRESS: predicted residual sum of squares, PRESS-ratio: averaged pointwise ratio of PRESS errors, NoiseVar: estimated variance of noise) for approximation of head-impact criteria in crashworthiness simulations (based on 42 points, 1000 DOEs). HIC – Head injury coefficient, HIC-d – head injury criterion, Corr – correlation coefficient, RMSE – root mean square error, MaxE – maximum error.

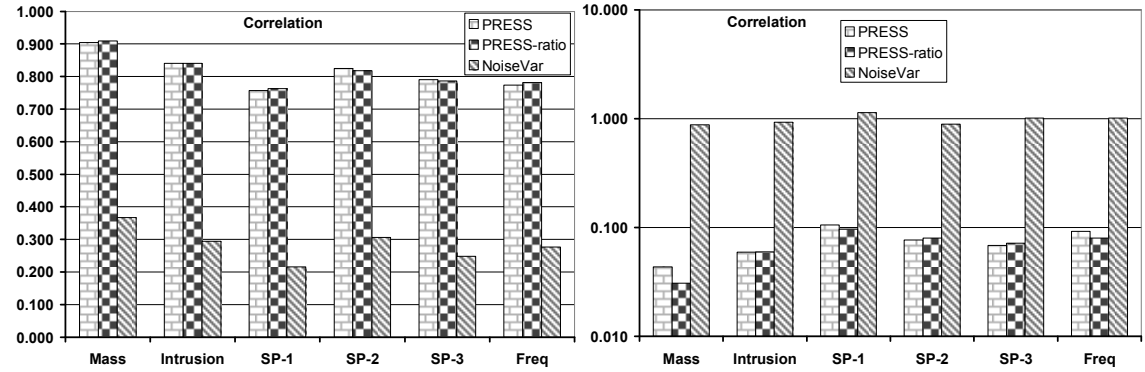

A) Mean – Correlation

B) Coefficient of variation – Correlation

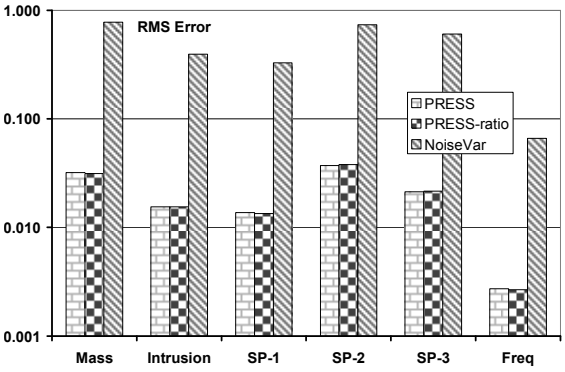

C) Mean – Root mean square error

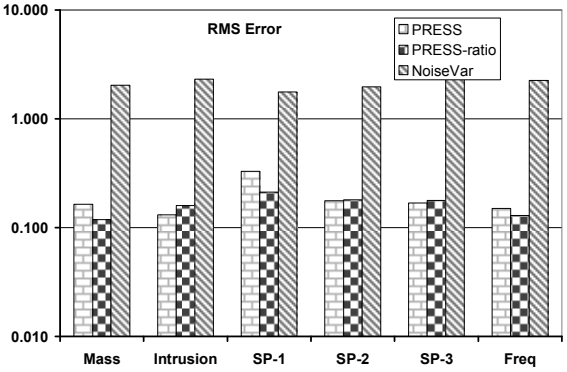

D) Coefficient of variation – RMSE

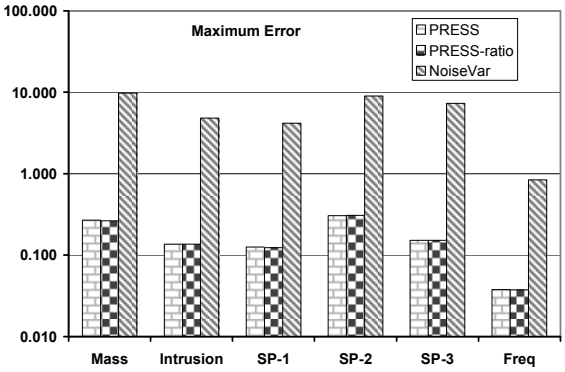

E) Mean – Maximum absolute error

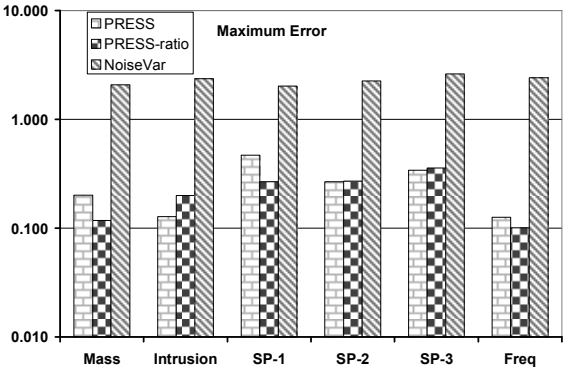

F) Coefficient of variation – Maximum absolute error

Figure 11. MDO crashworthiness example with reduced point density: Comparison of different RBF network topology selection criteria (PRESS: predicted residual sum of squares, PRESS-ratio: averaged pointwise ratio of PRESS errors, NoiseVar: RMS error) for approximation of responses in multidisciplinary crashworthiness simulation (based on 100 points, 1000 DOEs). SP-1 indicates Stage 1 pulse, SP-2 is Stage 2 pulse and SP-3 is Stage 3 pulse.

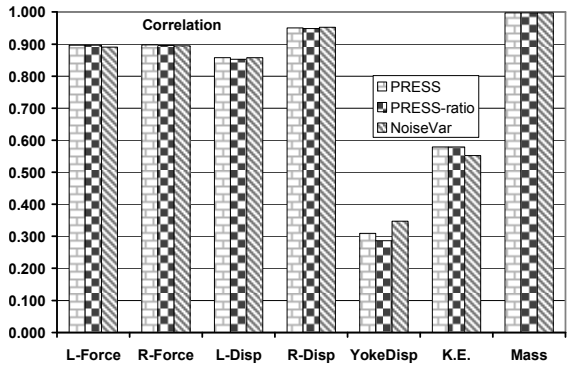

A) Mean – Correlation

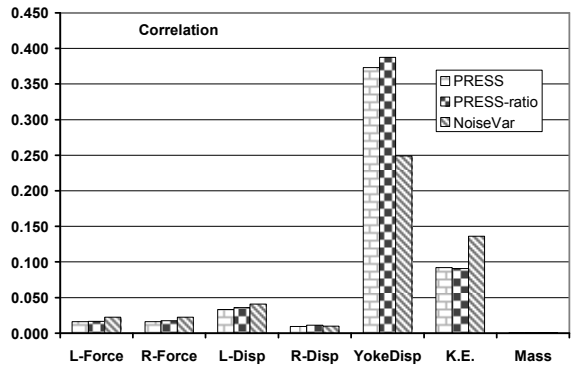

B) Coefficient of variation – Correlation

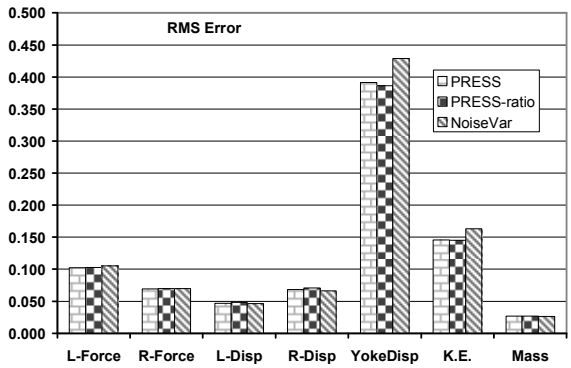

C) Mean – Root mean square error

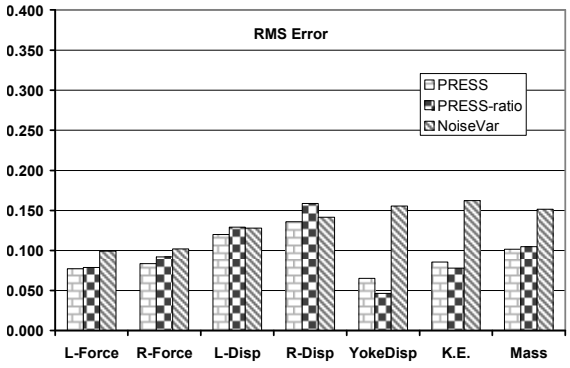

D) Coefficient of variation – RMSE

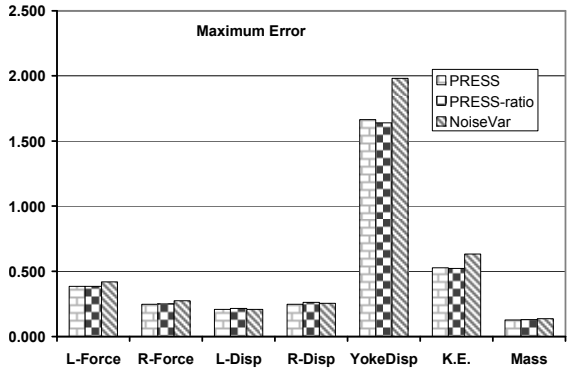

E) Mean – Maximum absolute error

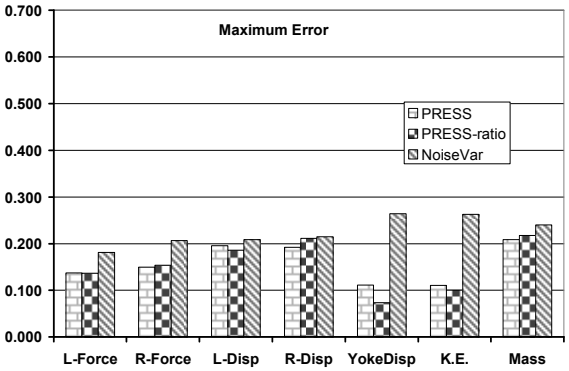

F) Coefficient of variation – Maximum absolute error

Figure 12. Instrument panel knee-impact analysis with reduced point density: Comparison of different RBF network topology selection criteria (PRESS: predicted residual sum of squares, PRESS-ratio: averaged pointwise ratio of PRESS errors, NoiseVar: RMS error) for approximation of responses in crashworthiness simulations of the automotive instrument panel structure knee-impact analysis (based on 50 points, 1000 DOEs).